Geo-Mar Lett (2003) 23: 34–42
DOI 10.1007/s00367-003-0122-5

Uwe Langrock · Ruediger Stein · Marcus Lipinski
Hans-Jürgen Brumsack

Paleoenvironment and sea-level change in the early Cretaceous Barents Sea—implications from near-shore marine sapropels

Received: 13 August 2002 / Accepted: 20 January 2003 / Published online: 4 April 2003

Abstract The late Volgian (early "Boreal" Berriasian) sapropels of the Hekkingen Formation of the central Barents Sea show total organic carbon (TOC) contents from 3 to 36 wt%. The relationship between TOC content and sedimentation rate (SR), and the high Mo/Al ratios indicate deposition under oxygen-free bottom-water conditions, and suggest that preservation under anoxic conditions has largely contributed to the high accumulation of organic carbon. Hydrogen index values obtained from Rock-Eval pyrolysis are exceptionally high, and the organic matter is characterized by well-preserved type II kerogen. However, the occurrence of spores, freshwater algae, coal fragments, and charred land-plant remains strongly suggests proximity to land. Short-term oscillations, probably reflecting Milankovitch-type cyclicity, are superimposed on the long-term trend of constantly changing depositional conditions during most of the late Volgian. Progressively smaller amounts of terrestrial organic matter and larger amounts of marine organic matter upwards in the core section may have been caused by a continuous sea-level rise.

Introduction

The late Jurassic–early Cretaceous time interval is characterized by low North Atlantic spreading rates which resulted in a relative sea-level low stand. This increased the prominence of shallow marine basins along the continental shelf, thereby promoting the development of restricted depositional environments, and favored the accumulation and preservation of organic matter (e.g., Demaison and Moore 1980). As a result, dark-colored, organic carbon-rich sediments, so-called black shales, occurred widely during this period, for example, in the marginal seas of the North Atlantic (e.g., Schlanger and Jenkyns 1976; Stein et al. 1986; De Graciansky et al. 1987), along the Norwegian–Greenland Seaway (e.g., Doré 1991; Smelror et al. 2001; Mutterlose et al. 2003), and in the adjacent Barents Sea (e.g., Bugge et al. 1989, 2002). The formation of black shales is often attributed to "oceanic anoxic events" (OEAs) on a global scale, for example, during the Cenomanian/Turonian which is characterized by a relatively high sea-level stand (e.g., Arthur et al. 1987; Erbacher et al. 2001).

The Cretaceous Barents Sea was located in a high paleolatitude realm (e.g., Haq et al. 1988; Hardenbol et al. 1998; Street and Brown 2000) and was dominated by fine-grained clastic sediments with thick black shale sequences (e.g., Worsley et al. 1988; Ziegler 1988). Some of these shallow marine black shales have received much commercial attention in the past because of their high petroleum source rock potential (e.g., Johansen et al. 1990; Larsen et al. 1990; Leith et al. 1990). Much of the scientific interest in these sequences was also raised by the Mjølnir meteorite (e.g., Gudlaugsson 1993; Dypvik et al. 1996), which impacted the paleo-Barents Sea close to the Volgian–Ryazanian (early/late Berriasian) boundary 142 ± 2.6 Ma ago (e.g., Smelror et al. 2001). Core 7430/10-U-01 is located only 30 km off the outer rim of the impact crater, and comprises the late Kimmeridgian to early Ryazanian Hekkingen Formation (e.g., Worsley et al. 1988; Bugge et al. 1989; Århus et al. 1990), of which the late Volgian sequence (cf. below for age control) shows an exceptional suite of organic carbon-rich, laminated black shales which are actually marine sapropels. The section from 47.65 to

U. Langrock (✉) · R. Stein
Department of Geosciences,
Alfred Wegener Institute for Polar and Marine Research,
Columbusstrasse, 27568 Bremerhaven, Germany
E-mail: ulangrock@awi-bremerhaven.de
Tel.: +49-471-48311571
Fax: +49-471-48311580

M. Lipinski · H-J. Brumsack
Institute for Chemistry and Biology of the Marine
Environments (ICBM), Carl von Ossietzky University,
26111 Oldenburg, Germany

46.85 meters below seafloor (m.b.s.f.) forms the so-called ejecta unit assigned to the meteorite impact (e.g., Dypvik et al. 1996), but there are new indications which suggest that the impact may have occurred much earlier, probably below 50 m.b.s.f. (Smelror et al. 2001). To obtain information about the origin of the late Volgian sapropels of core 7430/10-U-01 and their relation to paleoenvironmental and sea-level changes, as well as their possible relation to the Mjølnir meteorite impact, a detailed organic geochemical and microscopic study was performed.

Materials and methods

Geochemical and microscopic investigations were carried out on selected samples from the organic carbon-rich Hekkingen Formation of core 7430/10-U-01. The core was taken at 74°13′N and 30°14′E on the Bjarmeland Platform in the central Barents Sea north of the Nordkap Basin (Fig. 1) in a water depth of 335 m, and penetrated 57.10 m of late Jurassic to early Cretaceous bedrock. The drilling was performed by Sintef Petroleum Research in Trondheim, Norway (former IKU) in the year 1989. Total carbon (TC), total organic carbon (TOC), total nitrogen (TN), and total sulfur (TS) were measured on 148 samples after combustion using LECO CS-240 and CNS-2000 elemental analyzers, including 126 samples of a high-resolution section from 51 to 49 m.b.s.f. TOC was measured on a LECO CS-400 after carbonate was removed with hydrochloric acid. All TOC results were rechecked by CaO (total inorganic carbon TIC) determination on a CM-5012 CO2 coulometer (e.g., Engleman et al. 1985), using the equation TOC = TC − TIC. Estimates for quantity, quality, and maturity of the organic matter (OM) were drawn from hydrogen index (HI) values, oxygen index (OI) values, S2 values, and T_{MAX} values obtained from Rock-Eval pyrolysis (cf. Espitalié et al. 1977; Peters 1986). HI and OI signatures allow a rough distinction between algal/marine (types I and II kerogen) and woody/terrestrial (types III and IV kerogen) organic matter. Properties of particulate organic matter, such as type, abundance and degree of preservation, can provide most valuable information about sources (marine, lacustrine, or terrigenous) and conditions under which the OM was deposited (oxic, dysoxic, or anoxic).

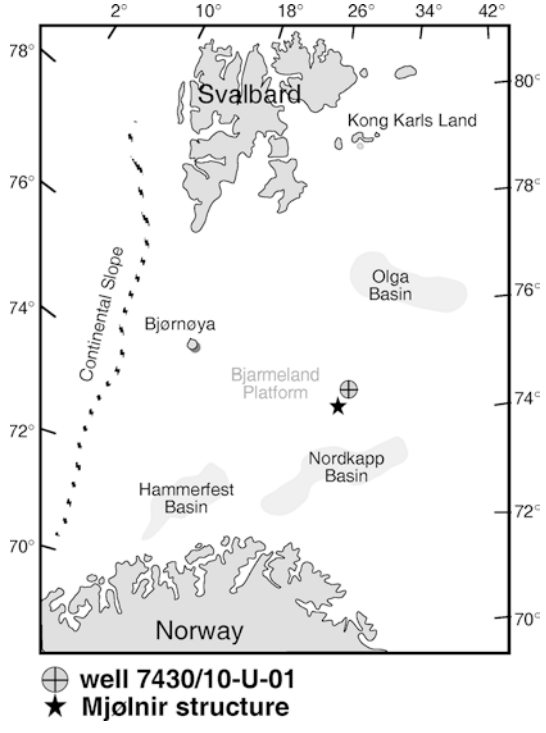

Fig. 1 Location of IKU well 7430/10-U-01 on the Bjarmeland Platform in the western central Barents Sea (335-m water depth)

For a more detailed qualitative and quantitative determination of the particulate organic matter, a petrographic analysis on 15 selected whole-rock samples was conducted by reflected light microscopy using white and fluorescent light. For statistical accuracy, at least 300 macerals were counted in each sample using a 25-point crosshair grid. We can generally distinguish between terrestrial (vitrinite, vitrodetrinite, inertinite, sporinite, and resinite) and marine/aquatic macerals (alginite, liptodetrinite, and acritarchs/dinocysts), following largely the nomenclature described in Taylor et al. (1998). For example, vitrinite and inertinite are derived from relatively hydrogen-poor (woody) land-plant remains, whereas sporinite is a collective term for spores and pollen which, although originating from terrestrial sources, may contribute to a relatively nitrogen- and hydrogen-rich sediment. Resinite is a product of waxy, fatty, or oily substances which also originate from land plants. Alginite, on the other hand, may be differentiated in marine (e.g., marine prasinophytes), more cosmopolitan (e.g., dinocysts and acritarchs), or freshwater genera (e.g., *Botryococcus*), which commonly produce hydrogen-rich types I and II kerogens. Particles smaller than 5 to 10 μm are given the suffix ''detrinite'', but is often hard to specify their origin.

In addition to the organic matter, all major and trace elements were determined by XRF and/or ICP-MS analysis (see Mutterlose et al. 2003), but in this paper only Mo/Al ratios were used to indicate bottom-water anoxia. To support this, pyrite size distribution is used for evaluating bottom-water redox conditions in ancient sedimentary rocks (e.g., Wilkin et al. 1996, 1997). Framboidal pyrite in sediments of modern anoxic basins, for example, the Black Sea, are typically smaller and less variable in size than those in sediments underlying an oxic or dysoxic water column. A semi-quantitative analysis on five samples was carried out under the microscope to determine the proportion of framboidal pyrite in the total amount of pyrite, and its size distribution.

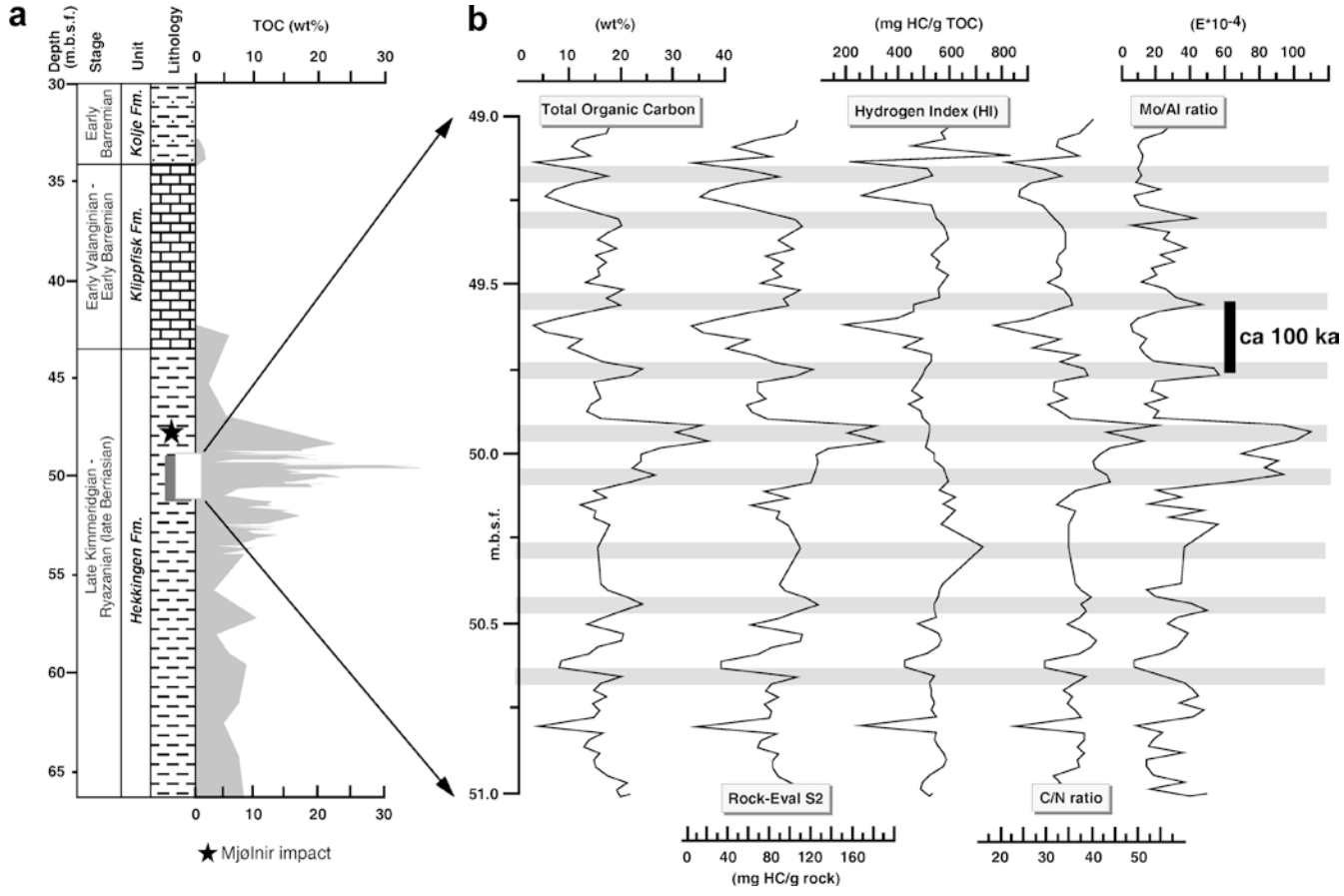

Fig. 2a Core depth, stratigraphic correlation (e.g., Gradstein et al. 1995; Smelror et al. 1998), lithology and regional formational limits of core 7430/10-U-01 showing TOC contents of the whole core, and a high-resolution sequence (extracted *box*). **b** High-resolution section from 51 to 49 m.b.s.f. showing down-core variations in TOC content, Rock-Eval S2 and HI values, and C/N and Mo/Al ratios. Maximum peaks are highlighted by *shaded lines*. Spacing between peaks may represent approx. 100 ka, revealing changing sedimentation rates (based on 0.2 cm per 1,000 years)

Results

The Hekkingen Formation core has TOC contents which vary widely from 5 to more than 20 wt%, with a prominent maximum of 36 wt% at about 50 m.b.s.f. (Fig. 2a; Table 1). There is a continuous increase towards this maximum, followed by a similar decrease (Fig. 2b). The late Volgian–early Ryazanian section (51–49 m.b.s.f.) was investigated in greater detail by high-resolution analyses (118 of the total 144 samples) to elucidate what may have caused and controlled the dramatic increase in organic carbon enrichment and preservation. To obtain information about the type of organic matter, several independent parameters were considered, including C/N ratios, HI and OI values, and especially maceral composition. Results of TOC content, Rock-Eval S2 and HI values, C/N and Mo/Al ratios are compiled in Fig. 2b, and all show a high positive correlation. C/N ratios range from 20 to 50, which would commonly indicate a strong terrestrial signal in the case of modern sediments (see below). Mo/Al ratios are very high ($10–40 \times 10^{-4}$) compared to average shale (e.g., Wedepohl 1970), and approach maximum values of 120×10^{-4} where all parameters reveal their maximum. HI values of 400–600 mg HC/g TOC and low OI values (≤ 20 mg CO_2/g TOC) were plotted as a van Krevelen-type diagram (Fig. 3), which indicates predominantly types I and II kerogen with a very good source rock potential for oil (cf. Espitalié et al. 1977; Peters 1986). Thermal immaturity of the organic matter is evident in T_{MAX} values of 410–430 °C (Langrock and Stein 2001; Mutterlose et al. 2003).

The maceral compositions of the sediments are dominated by lipid-rich organic matter derived from different marine/aquatic sources (Fig. 4), supporting the type II kerogen characterization by Rock-Eval pyrolysis. Massive occurrences of well-preserved marine Prasinophycean algae (mainly *Leiosphaeridia*), minor abundance of juvenile *Botryococcus*-type algae (freshwater), a few *Tasmanites*-type algae (brackish), and *Reinschia*-type algae (freshwater puddle) as well as a few low-diversity dinocysts (or acritarchs) were recorded at various depths. The terrigenous organic matter is mainly composed of terrestrial liptinite (sporinite and resinite), which may also contribute to the high HI values. Inertinite, vitrinite, and clasts of bituminous coal are less abundant. However, vitrinite and inertinite particles are occasionally up to 150 μm in length and well preserved. Most inertinite may

Table 1 Bulkgeochemical and Rock-Eval data of core 7430/10-U-01 (148 samples), including the high-resolution section from 51 to 49 m.b.s.f. (122 samples). Data are also shown in Fig. 2a, b

Depth (m.b.s.f.)	TOC (wt%)	C/N	HI[a]	OI[b]	S2[c]	T_{MAX} (°C)	Mo/Al ($\times 10^{-4}$)
32.82	0.9	8	27	218	0	427	0
33.98	1.9	22	47	117	1	441	1
34.46	0.1	3	29	*	0	420	1
36.33	0.0	1	167	*	0	341	1
37.64	0.0	4	28	*	0	427	8
38.73	0.0	2	*	*	*	*	3
39.74	0.0	1	135	*	0	535	2
41.17	0.0	1	364	*	0	527	2
42.62	0.1	1	24	*	0	393	2
43.10	5.7	18	620	40	36	425	14
45.65	2.9	17	225	55	6	424	2
47.26	5.4	23	422	32	23	420	14
48.72	22.9	29	407	18	93	417	32
49.11	17.6	40	611	7	107	424	27
49.13	17.5	39	598	8	105	426	29
49.15	16.7	37	570	8	95	424	24
49.17	11.3	33	580	10	66	424	13
49.19	9.9	32	454	11	45	426	10
49.21	13.6	37	839	9	82	425	13
49.23	2.9	21	209	10	6	421	12
49.25	11.4	29	512	12	58	420	10
49.27	16.9	33	535	9	91	422	12
49.29	10.6	27	447	11	48	420	9
49.31	6.6	24	332	15	22	423	23
49.33	4.8	24	258	21	13	425	8
49.35	9.9	29	529	12	52	425	11
49.39	19.1	32	549	16	105	423	43
49.41	19.5	33	572	10	112	422	6
49.43	16.8	34	590	16	99	427	28
49.45	14.8	*	591	14	88	426	25
49.47	18.6	34	557	14	104	426	38
49.49	14.5	32	524	19	76	426	23
49.51	16.6	32	559	13	93	424	31
49.53	15.1	33	546	10	82	423	18
49.55	15.4	33	595	14	92	422	21
49.57	12.5	30	571	14	71	424	12
49.59	19.9	34	555	13	111	427	26
49.61	16.8	35	558	12	93	424	32
49.63	19.3	36	460	2	98	414	47
49.65	12.9	31	460	2	60	428	22
49.67	7.0	27	391	5	27	426	10
49.69	2.5	19	188	20	5	424	6
49.71	4.8	25	345	6	16	430	7
49.73	12.1	33	493	3	60	430	15
49.75	9.3	27	417	6	39	426	11
49.77	12.5	37	528	3	66	429	14
49.79	16.1	33	524	3	84	430	19
49.81	23.8	38	509	3	121	429	54
49.83	21.3	39	496	5	106	433	57
49.85	14.1	32	480	5	68	427	20
49.87	15.1	31	456	4	69	428	18
49.89	15.5	34	494	1	77	429	27
49.91	13.5	30	437	5	58	426	14
49.93	13.1	33	484	3	63	425	22
49.95	15.7	35	495	3	78	427	19
49.97	35.1	54	520	2	183	432	93
49.99	30.1	43	518	1	156	429	110
50.01	36.5	51	516	1	189	428	101
50.03	27.2	44	504	2	137	432	82
50.05	23.3	42	538	2	126	429	70
50.07	23.4	40	541	1	127	433	91
50.09	21.8	40	576	1	125	431	83
50.11	26.1	43	*	7	*	*	94
50.13	21.4	44	593	3	120	426	67

Table 1 (Contd.)

Depth (m.b.s.f.)	TOC (wt%)	C/N	HI[a]	OI[b]	S2[c]	T_{MAX} (°C)	Mo/Al ($\times 10^{-4}$)
50.15	14.2	36	559	13	75	426	21
50.17	16.7	*	621	8	98	425	35
50.19	11.4	32	573	15	62	421	16
50.21	14.5	36	621	11	90	425	48
50.23	14.5	*	593	11	86	422	28
50.25	17.5	35	567	9	99	422	56
50.31	15.0	35	731	17	110	430	37
50.41	15.7	36	576	10	91	425	35
50.43	16.9	38	558	9	94	426	15
50.45	20.7	40	556	9	115	424	20
50.47	23.5	38	538	9	127	422	41
50.49	19.8	39	539	8	107	422	50
50.51	16.1	37	548	9	88	425	33
50.53	12.8	34	473	9	61	424	27
50.55	20.1	39	556	7	112	418	39
50.57	19.6	41	564	9	110	425	*
50.59	14.8	40	554	10	82	428	33
50.61	13.3	37	515	12	69	424	24
50.63	7.9	29	424	13	34	419	8
50.65	7.6	30	423	13	32	421	8
50.67	19.8	39	542	9	107	422	*
50.69	15.7	36	522	8	82	424	37
50.71	14.4	34	528	10	76	421	42
50.73	16.5	36	530	7	88	422	45
50.75	13.9	35	542	9	75	424	34
50.77	15.4	36	527	8	81	425	48
50.79	14.4	37	548	9	79	424	42
50.81	3.6	23	251	19	9	421	9
50.83	15.9	38	548	8	87	424	24
50.85	13.2	38	538	7	71	426	19
50.87	12.3	37	553	7	68	426	16
50.89	15.3	38	574	9	88	427	36
50.91	14.3	37	586	8	84	424	15
50.93	14.5	37	572	8	83	423	15
50.95	17.0	31	519	22	88	423	19
50.97	20.6	33	496	20	102	421	37
50.99	18.6	30	484	21	90	419	17
51.01	19.4	35	521	14	101	423	40
51.03	12.7	28	482	24	61	426	8
51.05	17.0	29	491	19	84	422	10
51.07	16.5	30	509	16	84	424	10
51.09	10.6	26	454	19	48	419	6
51.14	7.6	19	687	22	52	421	3
51.50	5.0	21	361	53	18	420	3
51.60	7.3	24	403	27	29	419	5
51.70	9.8	27	483	27	47	422	3
51.80	12.9	29	483	25	62	417	*
51.90	12.0	28	500	23	60	412	5
52.00	12.7	25	433	23	55	419	5
52.10	10.9	22	345	26	38	413	7
52.20	8.4	29	462	29	39	422	9
52.30	15.6	37	563	20	88	425	15
52.40	13.9	29	448	23	62	418	18
52.50	16.7	29	477	22	80	423	8
52.60	17.1	27	453	16	77	418	5
52.70	14.7	28	445	21	66	417	6
52.83	13.5	23	721	18	97	421	10
52.90	12.1	26	402	24	49	418	5
53.00	2.7	18	190	52	5	421	10
53.10	13.2	29	462	21	61	419	8
53.20	4.5	22	253	31	11	416	12
53.30	12.6	25	365	10	44	413	4
53.40	8.9	22	382	36	32	410	6
53.50	10.2	23	392	19	38	411	30
53.70	10.4	21	336	10	33	410	4
53.80	9.7	23	347	10	32	410	5

Table 1 (Contd.)

Depth (m.b.s.f.)	TOC (wt%)	C/N	HI[a]	OI[b]	S2[c]	T_{MAX} (°C)	Mo/Al ($\times 10^{-4}$)
53.88	8.2	22	406	8	32	413	3
53.90	5.8	21	269	2	15	411	15
54.00	7.8	24	408	7	30	414	15
54.10	7.6	*	471	13	34	416	7
54.17	3.5	25	168	18	6	408	447
54.28	8.6	23	458	22	40	419	4
54.30	10.0	23	449	17	43	413	3
54.55	4.4	24	228	*	9	408	225
54.60	8.3	25	492	*	38	420	8
56.50	3.5	17	520	60	18	426	1
57.90	10.3	26	521	33	54	423	2
58.79	4.1	18	347	32	14	417	2
59.74	5.9	19	447	24	26	416	11
60.34	8.6	25	452	24	39	424	10
62.35	7.5	25	344	16	26	421	2
63.36	5.3	21	343	14	18	428	1
65.15	7.4	28	158	26	12	428	0
67.20	8.2	23	418	32	34	422	17

[a]mg hydrocarbons per gram of TOC
[b]mg carbon dioxide per gram of TOC
[c]mg hydrocarbons per gram of rock

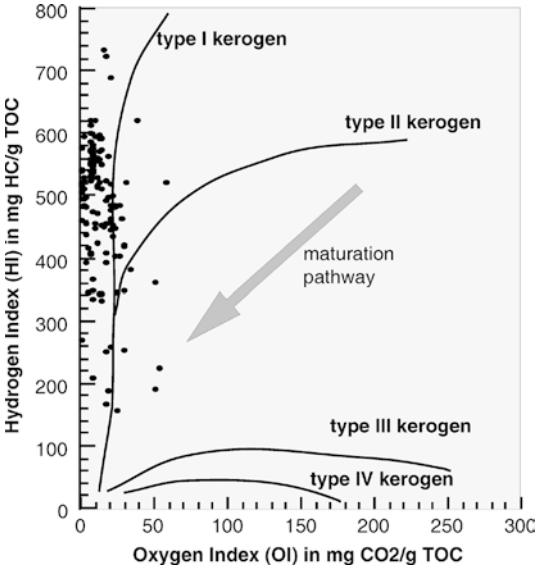

Fig. 3 Rock-Eval van Krevelen-type diagram shows dominantly type I and II kerogen, which may represent algal/marine OM of different preservation, or a mixture of fresh algal/marine and lipid-rich terrigenous OM (e.g., spores, resins)

be derived from charred plants (fusinites) and fungal spores (funginite). We particularly observed a continuous upward decrease of inertinite plus sporinite (which seem to be closely related in this case) along with an increase of marine-derived alginites (from about 60% at 52 m.b.s.f. to more than 95% at 50 m.b.s.f.). The amount of vitrinite and vitrodetrinite does not exceed 5% and remains relatively stable throughout this sequence.

A vast abundance (up to 15 vol% of the sediment) of small pyrite framboids appeared with diameters of 4 to 5 μm, implicating small absolute sizes and a low size variability.

In Fig. 2b the maximum peaks of all values appear in a more or less regular interval (shaded bars), which probably reflects some cyclicity. Based on a mean sedimentation rate of about 0.2 cm/1,000 years for the late Volgian (Smelror et al. 1998, 2001; Mutterlose et al. 2003), this frequency may represent the 100-ka orbital Milankovitch cycle. The different thickness of the intervals may then be a result of small variations in the sedimentation rate.

Discussion and conclusions

Depositional conditions

The causes for the deposition of organic carbon-rich sediments in Cretaceous marine environments has been controversial for a long time. Several authors favor basin-wide to global "stagnation" of deep waters, for example, deep basins with reduced vertical circulation which inhibits a renewal of water masses (e.g., Brumsack 1980, 1988; De Graciansky et al 1987). Others explain the occurrence of these black shales by an increased oceanic "productivity" which may lead to the formation of oxygen minimum layers which impinge on the seafloor (e.g., Schlanger and Jenkyns 1976). Furthermore, increased supply of terrigenous organic matter seems to be an important mechanism for the enrichment of organic carbon in some Mesozoic sediments (e.g., Stein et al. 1986; Stein 1991). However, contents of lipid-rich organic carbon in the sedimentary record as high as 36 wt% can hardly be explained without invoking a combination of elevated primary productivity, improved organic matter preservation, and limited dilution by clastic material from the continents.

The dark, laminated, and non-bioturbated sequence of core 7430/10-U-01 indicates a lack of benthic life and the absence of bottom-water oxygen, which inhibits a major part of the entire organic matter remineralization process which occurs at the sediment surface. In addition, the high amount of uniformly small, framboidal pyrite suggests that pyrite was almost exclusively formed within the water column. Consequently, not only the sediments surface but also at least part of the water column was (at least frequently) anoxic, which may have enhanced OM preservation. This situation is also reflected by the high TOC and HI values, and the abundance of well-preserved, autochthonous algal organic matter. The extraordinarily high Mo/Al ratios suggest that anoxic conditions extended beyond the sediment surface (e.g., Brumsack 1980, 1988; Mutterlose et al. 2003). The expansion of anoxia in the water column due to fluctuations in sea level and surface productivity may also lead to mass extinctions (e.g., Hallam and Wignall 1999), not only of primary producers but also of vast amounts of aerobic bacteria, that contributes to high TOC and HI values.

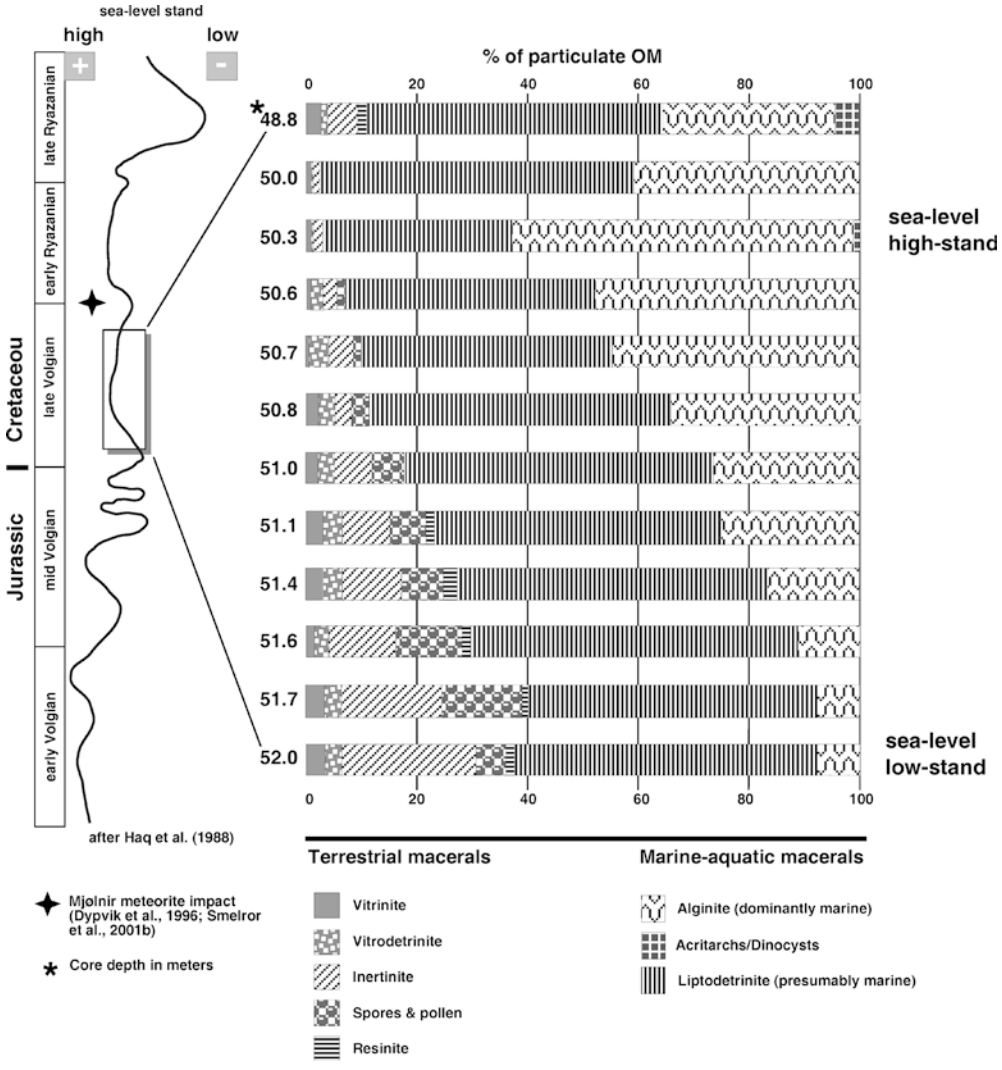

Fig. 4 Organic matter composition based on maceral analysis results versus depth (note this section ranges from 52 to 49 m.b.s.f.), and the correlation to the global sea-level curve suggested by Haq et al. (1988)

In recent and sub-recent marine environments, a high C/N ratio is often interpreted as an indicator for terrigenous (woody) organic carbon input (e.g., Stein 1991; Meyers 1997). In our case, however, the high C/N ratios correlate positively with the TOC, HI, and Mo/Al ratios, which are considered as indicators for marine (lipid-rich) OM and anoxia. Positive correlation between high TOC contents, marine organic carbon, and high C/N ratios is also reported from other organic carbon-rich sediments (e.g., Meyers 1997; Twichell et al. 2002), which may reflect enhanced paleoproductivity and/or improved preservation of OM. It is thereby considered that during sinking, partial degradation of algal OM may selectively diminish N-rich proteinaceous components, and raise the C/N ratio. This may, of course, be a direct response to enhanced primary productivity but probably requires greater water depths and a more oxic water column. Also, nitrogen can become strongly recycled if the supply of nutrients is limited (e.g., Waples and Sloan 1980), for example, in isolated stratified basins, which may also raise the C/N ratio. However, maceral analysis has clearly shown that high C/N ratios do not indicate an increased terrigenous input but instead likely reflect greater OM preservation due to anoxia.

Very low sedimentation rates in the late Volgian of core 7430/10-U-01 indicate that clastic dilution is strongly limited and that OM preservation was not controlled by rapid burial. In combination with very high TOC contents, deposition in the presence of anoxic bottom water is the most reasonable mechanism, rather than under conditions of high primary production (Fig. 5; e.g., Stein 1991). For a high primary productivity system, 10 to 50 times higher initial sedimentation rates would be required (according to Fig. 5). It is unlikely that such large amounts of carbonate were dissolved in the water column, because the average $CaCO_3$ content is still 10 wt%. It has also to be considered, however, that the age control on these sediments is very difficult, and that a long-term mean sedimentation rate has to be used. It can therefore not be excluded that periods of elevated primary productivity may also have occurred (along with the peak TOC values). This would have favored OM preservation by establishing an oxygen minimum zone (e.g., Arthur et al. 1987) probably

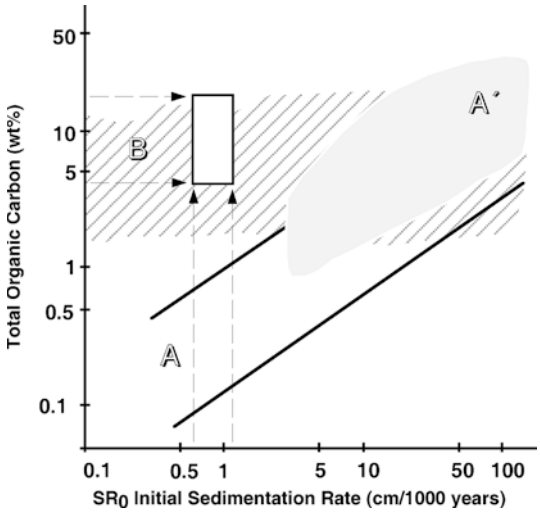

Fig. 5 TOC/SR_0 relationship diagram showing different fields of depositional conditions for marine sediments (after Stein 1990). *Field A* is characterized by a positive correlation between TOC content and sedimentation rate, indicating open, oxic deep-water conditions. *Field A′* indicates conditions of high oceanic primary productivity. *Field B* indicates anoxic depositional conditions where no correlation exists between TOC content and sedimentation rate. Sedimentation rates are given as initial (or decompacted) SR_0 (cf. Stein 1990 for details). The *open box* represents the field of most likely depositional conditions of the sequence investigated, based on minimum/maximum SR_0 (interpolated, estimated) and minimum/maximum TOC contents (measured)

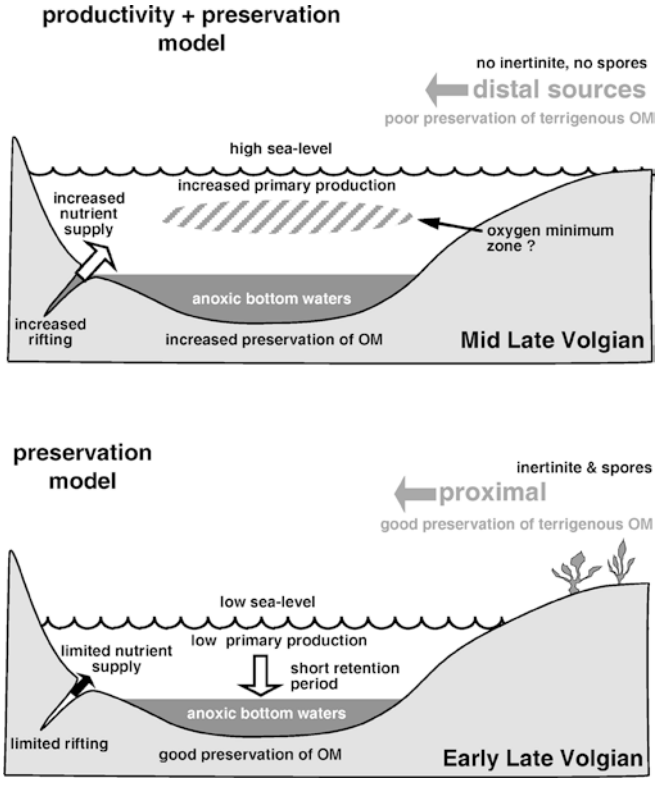

Fig. 6 Contrasting paleoenvironments and depositional conditions of the upper Hekkingen Formation best explained by the "preservation model" during low sea level (lower Late Volgian), and the "preservation + productivity model" during elevated sea level (upper Late Volgian)

extending over the entire water column (e.g., Sinninghe Damsté and Köster 1998).

Sea-level change

In order to evaluate an effect of a global sea-level change on the accumulation of organic carbon, the section 52–50 m.b.s.f. was investigated with a detailed microscopic analysis, because it is associated with a continuous change in the OM composition (Fig. 4). Over this depth interval, a decreasing amount of sporinite plus inertinite is apparent, which strongly suggests an increasing distance from their terrestrial sources (e.g., Littke et al. 1997; Taylor et al. 1998), probably associated with a sea-level rise (Fig. 6). Since the base of the sequence investigated (52.00 m.b.s.f.) is assigned to the base of the late Volgian (Smelror et al. 2001), the change in the OM composition can be correlated with the global sea-level curve postulated by Haq et al. (1988; Fig. 4). The upward-increasing amount of marine/aquatic alginite may reflect an increasing primary production which was promoted by the rising sea level (e.g., Sheridan 1987). Since the primary production is positively correlated with the "anoxia parameters", the variations are probably controlled by an additional preservation signal, probably caused by an expanded oxygen minimum zone. In summary, the remarkably high and increasing OM content in the late Volgian section from the Barents Sea (core 7430/10-U-01) was most likely caused by a combination of increasing preservation by bottom-water anoxia, coupled with periods of increasing primary production as well as a low and decreasing dilution of clastic material, which we relate to a marked rise in sea level.

Paleogeographic position

The analysis of the particulate organic matter provides strong evidence for a depositional environment in proximity to the paleoshore (Fig. 6) because high abundance of spores and pollen is typically found in near-shore marine and estuarine environments, and decreases substantially with increasing distance from land (e.g., Littke et al. 1997; Taylor et al. 1998). The occurrence of well-preserved algae (such as *Botryococcus* or *Pila*, *Tasmanites*, and *Reinschia* types) from freshwater and brackish habitats further points towards a near-shore environment. This is due to lipid-rich organic matter being more susceptible to biochemical degradation than, for example, inertinite, and it would therefore be less preserved if transported over greater distances (e.g., Littke et al. 1997). Furthermore, clasts of limnic coal facies (for example, bog-head coal) show good preservation and suggest a

short transport paths from their source. In addition, patchily distributed, coarse-grained minerals (apparently quartz) are found which are 60 to 200 μm in diameter. These minerals could not have been transported along with the claystone facies but only by another mechanism. Due to their patchy distribution, they may have been transported by episodic events, for example, storms, but they are too large to be transported far offshore (e.g., Füchtbauer 1988). However, there is another (although not yet proven) possible mechanism for the input of these large sand grains—by ice rafting. Episodes of a relatively cool climate were already suggested for the earliest Cretaceous Boreal realm (e.g., Price et al. 2000; Mutterlose et al. 2003), and another significant temperature drop was postulated for the Hauterivian Vocontian Basin at 30°N paleolatitude (e.g., Van de Schootbrugge et al. 2000). Hence, episodic (or even seasonal) IRD input can not be excluded for the late Volgian Barents Sea, which reveals a paleolatitude of almost 55°N.

According to previous paleogeographic estimates, the location of core 7430/10-U-01 was at least 300 km away from any coastline during the late Jurassic to early Cretaceous (e.g., Ziegler 1988; Bugge et al. 1989; Dypvik et al. 1996; Smelror et al. 1998). However, our results suggest a much more proximal position below wave base, which is indicated by the origin, the preservation, and the grain size of the organic material. During the relative sea-level low stand in the early late Volgian Barents Sea, tectonic highs and basin ridges may have emerged as land areas, separating a number of isolated, sediment-starved marine environments, as has been suggested for the Norwegian–Greenland Seaway (e.g., Doré 1991; Brekke et al. 1999). Although such areas may have provided little clastic input by rivers due to their limited sizes, they could have supported spore-producing land plants and freshwater habitats which eventually became the proximal sources for the organic matter of the upper Hekkingen Formation in the middle of the paleo-Barents Sea.

Influence by the Mjølnir meteorite impact

Our investigation provides a continuous geochemical and microscopic record of the upper Hekkingen Formation, and reveals no evidence for an impact event before 50 m.b.s.f. in core 7430/10-U-01. In view of exceptionally low sedimentation rates, drastic impact and/or post-impact effects caused by an impact of this dimension (see Gudlaugsson 1993; Dypvik et al. 1996) on the paleoenvironment, such as huge amounts of mobilized sediments, mass extinctions (e.g., Tsikalas et al. 1998), disturbance of water-column stratification, extinction of case-sensitive organic matter sources, etc., would have left distinct marks in the sedimentary record—which we have not detected.

Acknowledgements Financial support by the German Science Foundation (grant STE 412-13/1) is gratefully acknowledged. Sintef Petroleum Research, Norway, kindly provided access to sensitive core material and unpublished data. We thank Dr. Tom Wagner and two anonymous reviewers for their critical comments to improve the manuscript.

References

Århus N, Kelly SRA, Collins JSH, Sandy MR (1990) Systematic paleontology and biostratigraphy of two early Cretaceous condensed sections from the Barents Sea. Polar Res 8:165–194

Arthur MA, Schlanger SO, Jenkyns HC (1987) The Cenomanian-Turonian oceanic anoxic event. II. Palaeoceanographic controls on organic-matter production and preservation. In: Brooks J, Fleet A (eds) Marine petroleum source rocks. Geol Soc Spec Publ 26:401–420

Brekke HD, Dahlgren S, Nyland B, Magnus C (1999) The prospectivity of the Vøring and Møre basins on the Norwegian Sea continental margin. In: Fleet AJ, Boldy SAR (eds) Proc 5th Conf Petroleum Geology of Northwest Europe, 26–29 October 1997, London. Geol Soc Lond, vol 5, pp 261–274

Brumsack HJ (1980) Geochemistry of Cretaceous black shales from the Atlantic Ocean. Chem Geol 31:1–25

Brumsack HJ (1988) Rezente C_{ORG}-reiche Sedimente als Schlüssel zum Verständnis fossiler Schwarzschiefer. Habilitationsschrift, University of Göttingen

Bugge T, Elvebakk G, Bakke S, Fanavoll S, Lippard S, Leith TL, Mangerud G, Möller N, Nilsson I, Rømuld A, Schou L, Vigran JO, Weiss HM, Århus N (1989) (eds) Shallow drilling Barents Sea 1988. Trondheim, Norway, IKU rep

Bugge T, Elvebakk G, Fanavoll S, Mangerud G, Smelror M, Weiss HM, Gjelberg J, Kristensen SE, Nilsen K (2002) Shallow stratigraphic drilling applied in hydrocarbon exploration of the Nordkapp Basin, Barents Sea. Mar Petrol Geol 19(1):13–37

De Graciansky PC, Brosse E, Deroo G, Herbin JP, Montadert L, Müller C, Sigal J, Schaaf A (1987) Organic-rich sediments and paleoenvironmental reconstructions of the Cretaceous North Atlantic. In: Brooks J, Fleet A (eds) Marine petroleum source rocks. Geol Soc Spec Publ 26:317–344

Demaison GJ, Moore GT (1980) Anoxic environments and oil source bed genesis. Org Geochem 2:9–31

Doré AG (1991) The structural foundation and evolution of Mesozoic seaways between Europe and the Arctic. In: Channel JET, Winterer EL, Jansa LF (eds) Paleogeography and paleoceanography of the Tethys. Palaeogeogr Palaeoclimatol Palaeoecol 87:441–492

Dypvik H, Gudlaugsson ST, Tsikalas F, Attrep M Jr, Ferrell RE Jr, Krinsley DH, Mørk A, Faleide JI, Nagy J (1996) Mjølnir structure: an impact crater in the Barents Sea. Geology 24:779–782

Engleman EE, Jackson LL, Norton DR (1985) Determination of carbonate in geological materials by coulometric titration. Chem Geol 53:125–128

Erbacher J, Huber BT, Norris RD, Markey M (2001) Increased thermohaline stratification as a possible cause for an ocean anoxic event in the Cretaceous period. Nature 409:325–327

Espitalie J, Laporte JL, Madec M, Marquis F, Leplat P, Paulet J, Boutefeu A (1977) Source rock characterization method for petroleum exploration. In: Proc 9th Annu Offshore Technology Conf 3:439–443

Füchtbauer H (ed) (1988) Sedimente und Sedimentgesteine, Sediment-Petrologie Teil II, 4. Auflage. Schweizerbart, Stuttgart

Gradstein FM, Agterberg FP, Ogg JG, Hardenbol J, van Veen P, Thierry J, Huang Z (1995) A Triassic, Jurassic and Cretaceous time scale. In: Berggren, WA, Kent DV, Aubry MP, Hardenbol J (eds) Geochronology, timescales and global stratigraphic correlation. SEPM Spec Publ 54:95–126

Gudlaugsson ST (1993) Large impact crater in the Barents Sea. Geology 21:291–294

Hallam A, Wignall PB (1999) Mass extinctions and sea-level changes. Earth Sci Rev 48:217–250

Haq BU, Hardenbol J, Vail PR (1988) Mesozoic and Cenozoic chronostratigraphy and cycles of sea-level change. In: Wilgus CK, Hastings BS, Kendall CGStC, Posamentier HW, Ross CA, Van Wagoner C (eds) Sea level changes: an integrated approach. Soc Econ Petrol Mineral Spec Publ 42:71–108

Hardenbol J, Thierry J, Farley MB, Jacquin T, De Graciansky PC, Vail PR (1998) Mesozoic and Cenozoic sequence chronostratigraphic framework of European basins. In: De Graciansky PC, Hardenbol J, Thierry J, Vail PR (eds) Mesozoic and Cenozoic sequence stratigraphy of European basins. Soc Sediment Geol Spec Publ 60:7–14

Johansen SE, Ostisty BK, Birkeland Ø, Fedorovsky YF, Martirosjan VN, Bruun Christensen O, Cheredeev SI, Ignatenko EA, Margulis LS (1990) Hydrocarbon potential in the Barents Sea region; play distribution and potential. In: Vorren TO, Bergsager E, Dahl-Stamnes ØA, Holter E, Johansen B, Lie E, Lund TB (eds) Arctic geology and petroleum potential. Proc Norwegian Petroleum Society Conf. NPF Spec Publ 2:273–320

Langrock U, Stein R (2001) Organic matter preservation and paleoenvironmental implications for Lower Cretaceous marine sapropels from the Norwegian and Barents Sea shelf. European Union of Geosciences EUG XI J Conf Abstr 6:196–197

Larsen RM, Fjaeran T, Skarpnes O (1990) Hydrocarbon potential of the Norwegian Barents Sea based on recent well results. In: Vorren TO, Bergsager E, Dahl-Stamnes ØA, Holter E, Johansen B, Lie E, Lund TB (eds) Arctic geology and petroleum potential. Proc Norwegian Petroleum Society Conf. NPF Spec Publ 2:321–331

Leith TL, Weiss HM, Mørk A, Århus N, Elvebakk G, Embry AF, Brooks PW, Steward KR, Pchelina TM, Brø EG, Verba ML, Danyushevskaya A, Borisov AV (1990) Mesozoic hydrocarbon source-rocks of the Arctic region, In: Vorren TO, Bergsager E, Dahl-Stamnes ØA, Holter E, Johansen B, Lie E, Lund TB (eds) Arctic geology and petroleum potential. Proc Norwegian Petroleum Society Conf. NPF Spec Publ 2:1–25

Littke R, Baker DR, Rullkötter J (1997) Deposition of petroleum source rocks. In: Welte HD, Horsfield B, Baker DR (eds) Petroleum and basin evolution, insights from petroleum geochemistry. Geology and basin modeling. Springer, Berlin Heidelberg New York, pp 273–333

Meyers P (1997) Organic geochemical proxies of paleoceanographic, paleolimnologic, and paleoclimatic processes. Org Geochem 27:213–250

Mutterlose J, Brumsack HJ, Floegel S, Hay WW, Klein C, Langrock U, Lipinski M, Ricken W, Soeding E, Stein R, Swientek O (2003) The Norwegian–Greenland Seaway: a key area for understanding Late Jurassic to Early Cretaceous paleoenvironments. Paleoceanography (in press)

Peters KE (1986) Guidelines for evaluating petroleum source rock using programmed pyrolysis. Am Assoc Petrol Geol Bull 70:318–329

Price GD, Ruffell AH, Jones CE, Kalin RM, Mutterlose J (2000) Isotopic evidence for temperature variation during the Early Cretaceous (late Ryazanian–mid Hauterivian). Geol Soc Lond 155:335–343

Schlanger SO, Jenkyns HC (1976) Cretaceous oceanic anoxic events: causes and consequences. Geol Mijnbouw 55:179–184

Sheridan RE (1987) Pulsation tectonics as the control of North Atlantic paleoceanography. In: Summerhayes CP, Shackleton NJ (eds) North Atlantic paleoceanography. Geol Soc Spec Publ 21:255–275

Sinninghe Damsté JS, Köster J (1998) An euxinic southern North Atlantic Ocean during the Cenomanian/Turonian oceanic anoxic event. Earth Planet Sci Lett 158:165–173

Smelror M, Mørk A, Monteil E, Rutledge D, Leereveld H (1998) The Klippfisk Formation—a new lithostratigraphic unit of Lower Cretaceous platform carbonates on the Western Barents Shelf. Polar Res 17:181–202

Smelror M, Mørk A, Mørk MBE, Weiss HM, Løseth H (2001) Middle Jurassic–Lower Cretaceous transgressive-regressive sequences and facies distribution off Troms, northern Norway. In: Martinsen OJ, Dreyer T (eds) Sedimentary environments offshore Norway—Paleozoic to Recent. NPF Spec Publ 10:211–232

Stein R (1990) Organic carbon content/sedimentation rate relationship and its paleoenvironmental significance for marine sediments. Geo-Mar Lett 10:37–44

Stein R (1991) Accumulation of organic carbon in marine sediments. Springer, Berlin Heidelberg New York, Lecture Notes in Earth Sciences 34

Stein R, Rullkötter J, Welte DH (1986) Accumulation of organic-carbon-rich sediments in the late Jurassic and Cretaceous Atlantic Ocean—A synthesis. Chem Geol 56:1–32

Street C, Brown PR (2000) Paleobiogeography of Early Cretaceous (Berriasian–Barremian) calcareous nannoplankton. Mar Micropaleontol 39:265–291

Taylor GH, Teichmüller M, Davies A, Diessel CFK, Littke R, Robert P (eds) (1998) Organic petrology. Bornträger, Berlin

Tsikalas F, Gudlaugsson ST, Faleide JI (1998) Collapse, infilling, and postimpact deformation at the Mjølnir impact structure, Barents Sea. Geol Soc Am Bull 110(5):537–552

Twichell SC, Meyers PA, Diester-Haass L (2002) Significance of high C/N ratios in organic carbon-rich Neogene sediments under the Benguela Current upwelling system. Org Geochem 33:715–722

Van de Schootbrugge B, Föllmi KB, Bulot LG, Burns SJ (2000) Paleoceanographic changes during the early Cretaceous (Valanginian–Hauterivian): evidence from oxygen and carbon stable isotopes. Earth Planet Sci Lett 181:15–31

Waples DW, Sloan JR (1980) Carbon and nitrogen diagenesis in deep sea sediments. Geochim Cosmochim Acta 44(10):1463–1470

Wedepohl KH (1970) Environmental influences on the chemical composition of shales and clays. In: Ahrens LH, Press F, Runcorn SK, Urey HC (eds) Physics and chemistry of the Earth. Pergamon, Oxford, pp 307–333

Wilkin RT, Barnes HL, Brantley SL (1996) The size distribution of framboidal pyrite in modern sediments: an indicator of redox conditions. Geochim Cosmochim Acta 60(20):3897–3912

Wilkin RT, Arthur MA, Dean WE (1997) History of water-column anoxia in the Black Sea indicated by pyrite framboid size distributions. Earth Planet Sci Lett 148:517–525

Worsley D, Johansen R, Kristensen SE (1988) The Mesozoic and Cenozoic succession of Tromsøflaket. In: Dalland A, Worsley D, Ofstad K (eds) A lithostratigraphic scheme for the Mesozoic and Cenozoic succession offshore mid- and northern Norway. Norwegian Petrol Directorate Bull 4:42–65

Ziegler PA (1988) Evolution of the Arctic–North Atlantic and the western Tethys. AAPG Mem 43